



Labianca, C., Ferrara, C., Zhang, Y., Zhu, X., De Feo, G., Hsu, M., [You, S.](#), Huang, L. and Tsang, D. C. W. (2022) Alkali-activated binders — a sustainable alternative to OPC for stabilization and solidification of fly ash from municipal solid waste incineration. *Journal of Cleaner Production*, 380(Part 1), 134963. (doi: [10.1016/j.jclepro.2022.134963](https://doi.org/10.1016/j.jclepro.2022.134963))

There may be differences between this version and the published version.
You are advised to consult the published version if you wish to cite from it.

<https://eprints.gla.ac.uk/284952/>

Deposited on 8 November 2022

Enlighten – Research publications by members of the University of Glasgow
<http://eprints.gla.ac.uk>

1 **Alkali-activated binders – a sustainable alternative to OPC for stabilization**
2 **and solidification of polluting fly ash from municipal solid waste incineration**

3 Claudia Labianca¹, Carmen Ferrara², Yuying Zhang¹, Xiaohong Zhu¹, Giovanni De Feo², S.C
4 Hsu¹, Siming You³, Longbin Huang⁴, Daniel C.W. Tsang^{1,4*}

5

6 ¹Department of Civil and Environmental Engineering, The Hong Kong Polytechnic University, Hung Hom,
7 Kowloon, Hong Kong, China

8 ²Department of Industrial Engineering (DIIN), University of Salerno, via Giovanni Paolo II, 132–84084 Fisciano,
9 Italy

10 ³University of Glasgow, James Watt School of Engineering, Glasgow, G12 8QQ, UK

11 ⁴Sustainable Minerals Institute of University of Queensland, St Lucia QLD 4072, Australia

12

13 * Corresponding author: dan.tsang@polyu.edu.hk

14

15 **Abstract**

16 This research aims to evaluate the sustainability of alkali-activated binders for the
17 stabilization/solidification (S/S) of municipal solid waste incineration fly ash (MSWI FA). A
18 detailed environmental assessment of different alkali-activated mixtures was conducted using
19 life cycle assessment (LCA) to identify the factors affecting their environmental burden.
20 Ground granulated blast-furnace slag (GGBS) and metakaolin (MK) were used as the
21 precursors. Results showed that all the alkali-activated blocks fulfilled the requirements for
22 landfill and reuse as fill materials. Adopting alkali activation for S/S of MSWI FA instead of
23 OPC allowed up to 70% reduction of global warming potential. However, in other impact
24 categories such as human toxicity and land use, the alkali mixtures recorded higher values than
25 the mix with OPC (+60-70%), primarily because of the impacts related to the production of
26 chemical activators. The sensitivity analysis demonstrated that alternative production methods

27 for sodium silicate and sodium hydroxide could enormously reduce the impacts related to the
28 alkali solution. When the hydrothermal method for sodium silicate and the ODC method for
29 sodium hydroxide were adopted, a reduction of 71%, 22%, and 24% was recorded in global
30 warming potential, fossil resource scarcity, and human toxicity categories, respectively,
31 compared with the mix with OPC. Therefore, this study sheds light on alkali-activated materials
32 as sustainable S/S alternative to OPC to promote carbon neutrality.

33

34 **Keywords:** clinker-free treatment; Low carbon binder; Supplementary cementitious materials;
35 Hazardous waste management; Sustainable remediation; Incineration ash.

36

37

38 **List of abbreviations**

39 AAMs = Alkali-activated materials

40 APC = Air pollution control

41 BA = Bottom ash

42 DP = Diaphragm

43 FE = Freshwater eutrophication

44 FEcotox = Freshwater ecotoxicity

45 FPMF = Fine particulate matter formation

46 FRS = Fossil resource scarcity

47 FU = Functional unit

48 GC = GEOPOLYMER CONCRETE

49 GGBS = Ground granulated blast-furnace slag

50 GWP = Global warming potential

51 IR = Ionizing radiation

- 52 HT = Human toxicity
- 53 IWMF = Integrated waste management facilities
- 54 LCA = Life cycle assessment
- 55 LCI = Life cycle inventory
- 56 LCIA= Life cycle impact assessment
- 57 LU = Land use
- 58 MC = Mercury
- 59 MEcotox = Marine ecotoxicity
- 60 ME = Marine eutrophication
- 61 MK = Metakaolin
- 62 MM = Membrane
- 63 MRS = Mineral resource scarcity
- 64 MSW = Municipal solid waste
- 65 MSWI FA = Municipal solid waste incineration fly ash
- 66 ODC = Oxygen depolarized cathode
- 67 OPC = Ordinary Portland cement
- 68 PCDD/Fs = dibenzo-p-dioxins and dibenzofurans
- 69 POF = Photochemical oxidant formation
- 70 PTES = Potentially toxic elements
- 71 SOD = Stratospheric ozone depletion
- 72 S/S = Stabilization and solidification
- 73 TA = Terrestrial acidification
- 74 TCLP = Toxicity characteristic leaching procedure
- 75 TEcotox = Terrestrial ecotoxicity
- 76 WU = Water use

78 **1. Introduction**

79 Urbanization has led to a rapid growth of municipal solid waste (MSW) production. In China,
80 235.1 million tonnes of MSW were generated in 2020, with approximately 62% of which were
81 incinerated (China's Statistic Yearbook, 2020). Due to the forthcoming depletion of landfill
82 sites, incineration is considered as a preferred waste-to-energy approach that reduces the MSW
83 volume by 90% and improves the sustainability of waste management (Qiang et al., 2015; HK
84 EPD, 2018). MSW incineration (MSWI) commonly produces two main by-products, namely
85 MSWI bottom ash (BA) and MSWI fly ash (FA) (Zhang et al., 2021). In particular, MSWI FA
86 contains a high level of potentially toxic elements (PTEs) (lead, cadmium, chromium, mercury,
87 nickel, zinc etc.) and polychlorinated dibenzo-p-dioxins and dibenzofurans (PCDD/Fs) (Fan et
88 al., 2018), which leads it to be a hazardous waste. MSWI FA is collected before and after the
89 air pollution control (APC) system, and it accounts for about 3–15 wt.% of the original waste
90 total mass (Fan et al., 2018; Zhang et al., 2021). It is estimated that millions of tonnes of MSWI
91 FA are piled up in open landfills in China as a result of a lack of disposal companies, with
92 subsequent risks to the ecosystem (Xue and Liu, 2021). Therefore, there has been growing
93 concern regarding the adverse effects on human health and the environment resulting from the
94 disposal of MSWI FA (Li et al., 2019a). In addition, MSWI FA chemical composition can
95 extremely vary according not only to the type of incineration treatment, but also to geographical
96 and seasonal information.

97 China has launched the first technical specification about the management of MSWI FA (HJ
98 1134, 2020) pollution control in August 2020. If well-treated, MSWI FA can be considered as
99 one type of general waste and disposed in sanitary landfill, or even be used for other purposes
100 (GB 34330, 2017). Although the recycling of this material has not yet been globally regulated,
101 it is necessary to investigate sustainable alternatives for the MSWI FA disposal (GB 34330,

102 2017). Over the last few years, increasing attention has been paid to properly stabilize MSWI
103 FA for significantly lowering associated environmental risks at the final disposal site. So far,
104 the most widely accepted solution involves stabilization and solidification (S/S) with a variety
105 of hydraulic binders, such as cement, lime, blast furnace slag, etc. (Chen et al., 2019a; De Gisi
106 et al., 2020).

107 In the last 60 years, OPC-based S/S has been proven to be an economically efficient approach
108 to immobilize toxic and harmful pollutants in MSWI FA, through encapsulation, fixation, or
109 adsorption in hydration products resulting from chemical reactions between cement and water,
110 such as calcium silicate hydrates (C-S-H) gel and ettringite (AFt), (Contessi et al., 2020).
111 However, the durability of OPC-based S/S is significantly weakened by the poor compressive
112 strength of matrix encapsulating large proportions of MSWI FA. It is known that the high
113 chloride and sulfate contents in MSWI FA can adversely affect the strength and durability of
114 the final blocks (Xu et al., 2019). Guo et al. (2021) demonstrated a low compatibility of OPC
115 with oxyanions (e.g., AsO_3^{3-}) or amphoteric metal ions (e.g., Zn^{2+} , ZnO_2^{2-}), due to a significant
116 inhibition of the cement hydration caused by complexation reactions of calcium ions. Although
117 this weakness may be improved by increasing the proportion of OPC in the mix, it will lead to
118 the use of large amounts of cements and associated high costs. In addition, the production of
119 OPC creates tremendously high carbon footprint (0.66–0.82 t CO_2 per t OPC) (Dung and
120 Unluer, 2017), leading to a growing interest in alternative low-carbon binders. For each tonne
121 of Portland cement produced, approximately 1 kg of SO_2 , 2 kg of NO_x , and 10 kg of dust are
122 emitted (Singh et al., 2020). Among alternative binders, alkali-activated materials (AAMs)
123 have received increasing attention in recent years, especially for the possibility of recycling by-
124 product or waste materials from agricultural and industrial processes, but also for their
125 considerable chemo-mechanical performances. Jin et al. (2016) found that MSWI FA S/S based
126 on the use of metakaolin (MK) displayed excellent stability in acid and alkaline environments

127 and good performance as a building material with no secondary pollution. By entrapping
128 several components, such activation creates a cement-like matrix that drastically reduces
129 pollutant mobility. Furthermore, AAMs can guarantee a higher mechanical resistance than
130 traditional concrete (Chindaprasirt and Rattanasak, 2018). It has been suggested that the
131 properties of MK-based AAMs can be improved using other thermally activated clays with
132 higher Si/Al ratios or by combining with slag acting as a Ca-rich precursor (Davidovits, 2009).
133 Precursors derived from industrial and agricultural wastes may be used to lower the costs and
134 assist the waste disposal for sourcing process, such as ground granulated blast furnace slag
135 (GGBS), pulverized fuel ash, glass powder, palm oil fuel ash, rice husk ash, silica fume, and
136 marble powder rich in aluminate-silicate content. These wastes have been found to have a big
137 potential in S/S application via alkali-activation (Jeremiah et al., 2021). However, the relative
138 abundance of different waste varies, such as the limited availability if GGBS as a by-product
139 of the manufacture of pig iron from iron ore (Davidovits, 2009; Juenger et al., 2019). Other
140 industrial wastes and by-products (such as rice husk ash, silica fume, sodium aluminate slurry)
141 have great potential as sustainable activators in AAMs (Billong et al., 2021). Therefore, the
142 development of alternative materials or optimized binary mix designs must consider the
143 availability of wastes and their sources.

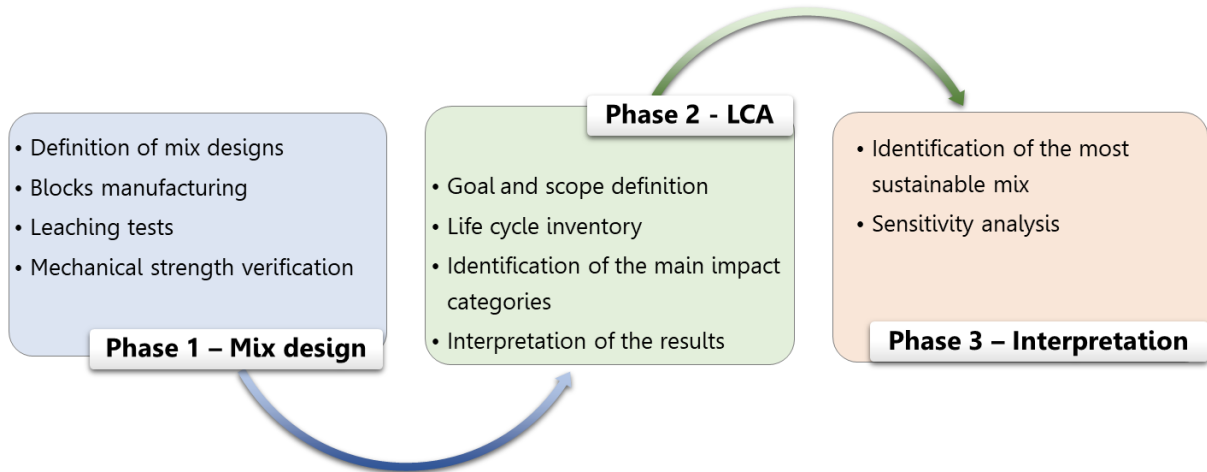
144 Evidence suggests that AAMs yield the best CO₂ reduction as of 26–45% compared to normal
145 OPC (Krivenko, 2017). McLellan et al. (2011) demonstrated that AAMs could significantly
146 reduce CO₂ emissions by up to 64% over OPC-based concrete. In a more recent study, the
147 global warming potential (100-years) of AAMs was 5–35% lower than PC concrete (Patrisia
148 et al., 2022). Nonetheless, there is some concern about the impacts related to the activator
149 solution used in the geopolymerization process, which are usually made as a combination of
150 silicates, hydroxides, and carbonates (Krivenko, 2017). Salas et al. (2018) identified sodium
151 hydroxide as the most relevant life cycle process in terms of carbon emissions, being used also

152 for sodium silicate production. In the studies by Robayo-Salazar et al. (2018) and Bajpai et al.
153 (2020) sodium silicate and sodium hydroxide contributed for 85% and 60% as total,
154 respectively, of the total emissions despite representing less than 9% in volume of the alkali-
155 activated concrete mixture. Sodium hydroxide and sodium silicate are the main constituents
156 responsible for 60% of total environmental impacts of geopolymer concrete (GC).
157 Therefore, the identification of the optimal mix design has a key role for the evaluation of the
158 life cycle assessment (LCA) of AAMs. The main strategy for a sustainable mix should focus
159 on minimizing the consumption of energy or raw materials and the generation of waste. The
160 objective of this study is to develop and identify the most sustainable alkali-activated mixture
161 design to stabilize MSWI FA, alternatively to OPC. Firstly, an experimental phase allowed
162 investigating the effectiveness and the compliance with the regulations of the S/S mix designs
163 under study. Then, a LCA-based evaluation explored the main impacts and identified the most
164 environmentally sustainable design. Through the sensitivity analysis, a focus on alternative and
165 more sustainable production methods for alkalis was essential. It is expected that the data
166 presented in this paper will assist industry stakeholders and researchers in getting a
167 comprehensive idea of the potential of using AAMs for MSWI FA S/S and spur environmental
168 responsibility actions.

169

170 **2. Method**

171 This research contains three main phases, as shown in Fig. 1. Phase 1 includes the preparation
172 and technical evaluation of different mixtures of alkali-activated S/S blocks, where the
173 combination of two different precursors (GGBS and MK) is considered. In Phase 2, the
174 environmental impacts of the S/S mix designs are evaluated and interpreted by employing
175 LCA. Lastly, Phase 3 aims to identify the best mix design for sustainability and technical
176 requirements.



177

178

Figure 1. Flowchart of the methodology used in this study.

179

180 **2.1 Materials and mix designs**

181 The MSWI FA used in this study was collected from the incinerator in Shenzhen, China.

182 GGBS and MK were used as the precursors, and sodium silicate and sodium hydroxide-based

183 solutions were chosen as the activators. All the chemicals and binders used were purchased

184 from Mainland China; instead, OPC was supplied by Green Island Cement Limited, Hong

185 Kong. The chemical compositions of raw materials are reported in Table S1 (Supplementary

186 Materials). Four different alkali mixtures were designed to investigate the efficiency and

187 sustainability of alkali-activated S/S treatment, as shown in Table 1. A conventional case

188 scenario with OPC was also considered as a comparison.

189

190 The alkali content and type are crucial for achieving satisfactory performance of AAMs, which

191 depends significantly on the selection of the precursor (Wang et al., 2015). Normally, the

192 aluminosilicate precursor with higher CaO content requires lower alkali content. For example,

193 GGBS is a typical high-Ca precursor for preparing AAMs, which requires only 4-7 wt.% alkali

194 content (R_2O eq.%) for strong alkalis (R stands for alkali metals) (Wang et al., 2015). However,

195 MK needs more alkalis (> 10 (R_2O eq.) wt.% alkali content (Sun et al., 2020)) due to the lack
 196 of CaO (Rashad, 2013). If the water glass (i.e., sodium silicate, $R_2O \cdot (n)SiO_2$) is used for
 197 producing AAMs, a modulus (n) of 1.0-2.0 is normally chosen for the optimised properties (Li
 198 et al., 2019b; Provis et al., 2019). The suitable concentration of water glass ($M_s = 1.0$) is the
 199 alkali activator that we used in this study. Therefore, the alkali content in this study is
 200 proportionally designed based on those existing studies, i.e., 5~8 wt.% for GGBS and 10~13
 201 wt.% for MK. In addition, a small amount of alkali (0 ~ 1 wt.%) was assigned to MSWI FA to
 202 activate the aluminosilicates contained in it to enhance the S/S efficiency. The MSWI FA
 203 content was fixed as 75 wt.% of the total solid binder in the mixtures, and the remaining 25
 204 wt.% was either MK, GGBS, and OPC or the mixture of them (Table 1). Two binary systems
 205 were also considered with the GGBS:MK ratio equal to 9:1 and 7:3. The conventional S/S with
 206 OPC (M5) was designed according to Eq. 1 (Chen et al., 2022) for achieving a suitable
 207 workability of paste:

$$Water (wt. \%) = OPC (wt. \%) \times 0.4 + MSWI FA (wt. \%) \times 0.45 \quad Eq. 1$$

209
 210 **Table 1.** Mix design for S/S of MSWI FA (wt.%).

	Mix design	MSWI FA	GGBS	MK	Sodium silicate	Sodium hydroxide	OPC	Water
M1	MSWI FA + GGBS	51.55	17.18	-	1.22	0.77	-	27.49
M2	MSWI FA + MK	49.68	-	16.56	1.49	5.79	-	26.49
M3	MSWI FA + GGBS + MK (9:1)	51.36	15.41	1.71	3.29	0.84	-	27.39
M4	MSWI FA + GGBS + MK (7:3)	50.97	11.89	5.10	3.86	0.99	-	27.18

211

212 **2.2 Samples preparation and characterization**

213 The block production process involved solution preparation, dry and wet mixing of powders,
214 casting, and curing phases. In the mixing phase, binders and MSWI FA were dry-mixed for 2
215 min, and then the activator solutions were added for another 3-min mixing to obtain a
216 homogeneous paste. In the casting phase, fresh alkali-activated pastes were poured into 20 x
217 20 x 20 mm steel molds. All samples were demolded after 2 days, wrapped in a waterproof
218 membrane, and kept at 23 ± 2 °C in a curing chamber for up to 28 days and 60 days. All the
219 experiments on S/S blocks were in triplicates for quality assurance. The 28-d and 60-d uniaxial
220 compressive strength of the S/S blocks was tested using a universal testing machine
221 (Testometric CXM 500-50 KN) and the loading rate was 0.5 mm s^{-1} according to BS EN
222 12390-3 (2019). The leachability of PTEs together with the pH was tested according to the
223 Toxicity Characteristic Leaching Procedure (TCLP) (US EPA, 2019). The leaching
224 concentrations of PTEs were detected by inductively coupled plasma atomic emission
225 spectrometry (ICP-AES, Spectro Arcos). Further details of the procedure can be found in Wang
226 et al. (2019).

227

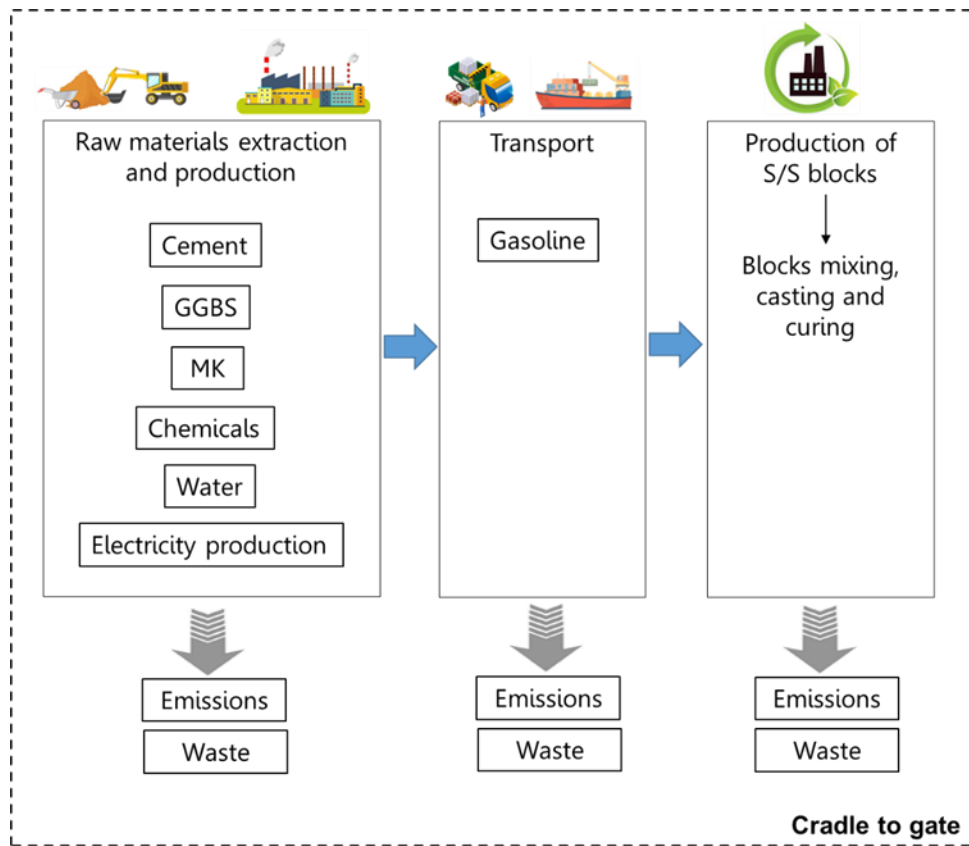
228 **2.3 LCA study**

229 **2.3.1 Goal and scope**

230 The goal of the study was to comparatively evaluate the environmental life cycle impacts
231 associated with the different S/S mix designs for MSWI FA treatment defined in Section 2.1
232 to identify the most environmentally sustainable alternative. Following the guidelines provided
233 by ISO 14040 (ISO, 2006), the LCA was performed according to a cradle-to-gate approach.
234 The new Integrated Waste Management Facilities (IWMF) constructed in Hong Kong on an

235 artificial island near Shek Kwu Chau were considered as the case study (HK EPD, 2022). The
 236 boundaries for the system included the raw materials extraction, processing, transport, and the
 237 S/S block production (Fig. 2) for all the scenarios considered. The end-of-life was not included
 238 in this study being similar for all the scenarios. In agreement with other LCA studies on the
 239 topic, the functional unit of the study was defined as 1 m³ of final product containing MSWI
 240 FA (Colangelo et al., 2021; Hossain et al., 2021) as it is more representative. An averaged
 241 density (Table S2) was considered to facilitate data management and application as all the
 242 mixes had similar density values (Colangelo et al., 2021). Furthermore, it should be noted that
 243 the different types of S/S mixtures had comparable mechanical properties, workability, and
 244 durability performance and they all accomplished the standard technical requirements for on-
 245 site landfill use as fill materials (HK EPD, 2011).

246



247

248

Figure 2. System boundaries of the studied S/S blocks.

249

250 **2.3.2 Life cycle inventory**

251 For this LCA step, all relevant aspects of energy and mass flow, as well as emissions to air,
252 water and land were collected for each unit process and normalized to the functional unit of the
253 study. The modeling of the proposed AAMs- and conventional cement-based S/S treatments
254 was performed using the SimaPro[®] software v. 9.0049 to model products and processes
255 comprehensively and analyze the results interactively (PRé Consultants, 2019). All the data
256 considered for the material and energy flows were obtained from both laboratory analyses
257 (primary data) and Ecoinvent v. 3.3 database or scientific literature (secondary data). In
258 particular, secondary data were considered for the upstream flows, from the extraction of raw
259 materials to their processing phase, and primary data were used for the production of S/S blocks.
260 To ensure regionally specific results, local data were used to the maximum extent possible.

261

262 The weight values of all components contained in each MSWI FA S/S block can be obtained
263 from the data reported in Table 1, considering the total weight of the blocks (Table S2). A
264 variety of materials along with their processing and transport are required for the
265 comprehensive assessment of all scenarios. Considering Hong Kong's limited resources,
266 construction materials are mainly imported from Mainland China or other countries (Hossain
267 et al., 2019). For all the scenarios, the transport distances were calculated from each material
268 production site to the block manufacturing location in Hong Kong. A preliminary screening of
269 possible suppliers showed several available options in the Guangdong province from where all
270 the required materials can be shipped by barge to the artificial island where the new IWMF in
271 Hong Kong is located. Table 2 lists the imported materials as well as their distances and modes
272 of transport. Table 3 shows the amount of energy consumed during S/S block production.
273 GGBS is a by-product of iron making; however, in Ecoinvent database v. 3.3 the entire

274 production process of GGBS is available with all emissions and resources included. For MK,
 275 the database Ecoinvent was used jointly with literature data (Habert and Ouellet-Plamondon,
 276 2016). MSWI FA was considered to be burden-free since the objective of the study was to
 277 identify the best mix design to stabilize MSWI FA and no avoided impacts of landfill disposal
 278 were considered.

279

280

Table 2. Distances and modes of transport used in this study.

Materials	Imported from	Transport type (t)	Distance
GGBS	Zhanjiang, Guangdong Province, China Maoming port, China	Inland waterways barge	240 NM
MK	Maoming port, Guangdong Province, China	Inland waterways barge	180 NM
OPC	Local supplier in Hong Kong	- Lorry (16-32 t) - Inland waterways barge	27 km 13 NM
Sodium hydroxide	Canton, Guangdong Province, China	Inland waterways barge with reefer machine	75 NM
Sodium silicate	Sanshui Foshan, Guangdong Province, China	Inland waterways barge with reefer machine	100 NM

281

282

Table 3. Materials and energy requirements used in this study.

Material	Upstream data source
MSWI FA	Burden-free
GGBS	Ecoinvent
MK	Ecoinvent + Literature
OPC	Ecoinvent

Sodium hydroxide	Ecoinvent (Sodium hydroxide in 50% solution state, membrane cell)
Sodium silicate	Ecoinvent (Sodium silicate in 37% solution state)
Deionised Water	Ecoinvent
Lorry (16-32 t)	Ecoinvent
Lorry with refrigerator machine (7.5-16 t)	Ecoinvent
Inland barge	Ecoinvent
Inland barge with refrigerator machine	Ecoinvent
Electricity country mix	Ecoinvent (Electricity, medium voltage CN)
Heat	Ecoinvent
Processes	Energy requirement
AAMs Block making process	7 kWh (8 min mixing)
Solution preparation	6 kWh (4 h mixing)
OPC Block making process	5.5 kWh (6 min mixing)

283

284

285 **2.3.3 Life Cycle Impact Assessment**

286 The LCA analysis was performed using ReCiPe 2016 (H), in which the key issues were
287 assessed from a hierarchical perspective based on midpoint (problem oriented) and endpoint
288 (damage oriented) indicators (Huijbregts et al., 2017). There are 22 categories in the endpoint
289 approach, which are classified into three macro-areas: Human health (measured in terms of
290 disability adjusted life years, DALYs), Ecosystems (measured in terms of species × year), and
291 Resources (measured in terms of USD 2013) (Huijbregts et al., 2017). Both levels of the
292 method were used to assess the impacts, and the results describe both midpoint and endpoint
293 indicators. However, the most representative midpoint categories were considered for further

294 discussion. In such cases, only the categories that contributed the most to the endpoint level
295 were chosen, as defined by Cleary (Cleary, 2013). In particular:

296 - Global warming potential (GWP, kg CO₂eq) that evaluates the integrated infrared radiative
297 forcing increase of greenhouse gas (GHG).

298 - Particulate matter formation (PMF, kg PM_{2.5}eq) that considers the air pollution that causes
299 primary and secondary aerosols in the atmosphere.

300 - Fossil resource scarcity (FRS, kg oileq) that considers the fossil fuel potential, defined as the
301 ratio between the higher heating value of a fossil resource and the energy content of crude oil.

302 - Land use (LU, m²a) that focuses on the relative species loss due to local land transformation,
303 land occupation, and land relaxation.

304 - Human toxicity (HT, kg 1,4-DBeq) that accounts for the environmental persistence (fate),
305 accumulation in the human food chain (exposure), and toxicity (effect) of a chemical.

306 - Water use (WU, m³) that calculates the water consumed and not available anymore in the
307 watershed for humans nor for ecosystems.

308

309 **3. Results and discussion**

310 **3.1 Compressive strength and leachability**

311 The density (Table S2) and compressive strength of the investigated pastes were experimentally
312 measured. A barely perceptible difference can be observed in the density of S/S blocks because
313 MSWI FA accounts for 75 wt.% in the final matrix. Regarding the compressive strength of
314 AAMs, all the blocks complied by far with the strength requirement (1 MPa) for on-site use as
315 fill materials (HK EPD, 2011) (Fig. 3a). Compared to the mix with MK, the mix with GGBS
316 performed better with an increase of 20% and 31% of the final compressive strength at 28 and
317 60 days, respectively. This can be allocated to the fact that in the calcium-containing binder,
318 calcium silicate hydrate/calcium aluminosilicate hydrate (C-S-H/C-A-S-H) seeds can serve as

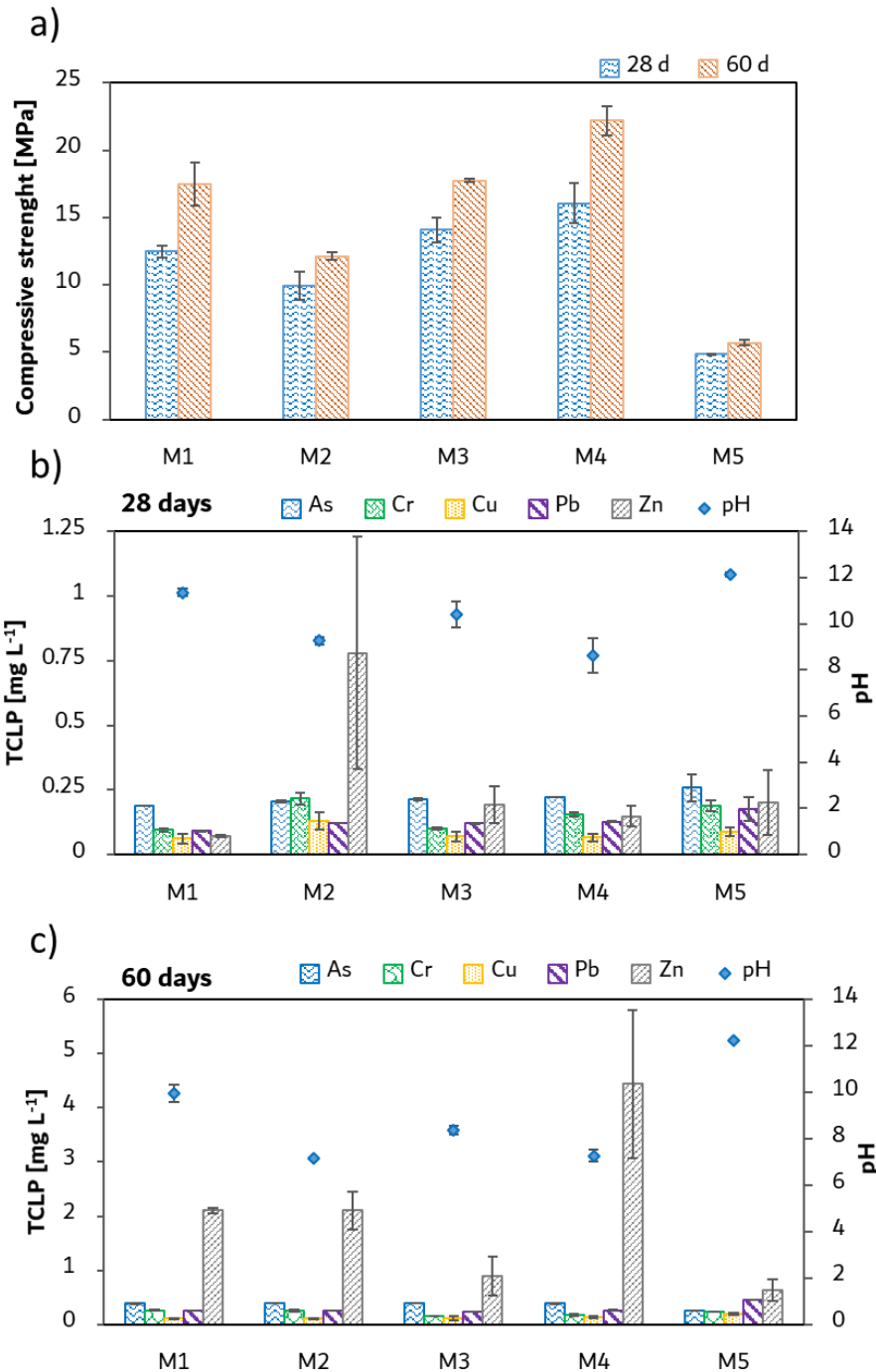
319 nucleation sites to promote the formation of geopolymer gel (Yip and Van Deventer, 2003;
320 Puligilla et al., 2019).

321 However, the combination of GGBS with MK in a 7:3 weight ratio developed final mechanical
322 strength higher than single-binder mixes, in particular an increase of 21%, 45%, 20% than mix
323 M1, M2, and M3 was recorded, respectively. Yet the compressive strength was higher than 10
324 MPa in all scenarios with peaks of 22.18 MPa and 17.46 MPa for M4 and M1, respectively.
325 The mix M5 with 25% OPC showed a compressive strength at 28-d lower than the AAM
326 blocks, particularly 61%, 51%, 66%, and 70% lower than M1, M2, M3, and M4, respectively.
327 At 60-d this difference was even stronger, as it is shown in Fig. 3. This outcome was in line
328 with the studies by Chen et al. (2019b; 2022) on OPC-based S/S and it underlines the great
329 potential of geopolymerization technology for diverting hazardous wastes from disposal to
330 reuse in engineering applications where a much higher mechanical strength can be reached
331 (Hossain et al., 2020).

332

333 The immobilization efficiency must fulfill the leachability limits. At this regard, all the mixes
334 complied not only with the "Landfill Disposal Criteria" (HK EPD, 2011) but also with the
335 "Universal treatment standards for on-site reuse of cement stabilization/solidification treated
336 soil" in Hong Kong (HK EPD, 2011) (Fig. 3b-c). The TCLP leachability results of untreated
337 MSWI FA is shown in Table S3. The pH ranges from 8 to 11 for alkali-activated mixes, falling
338 within the optimum 5–11 range proposed by Yakubu et al. (2018), as most PTEs can be
339 effectively solidified/stabilized within this range. The mix with GGBS reached more alkaline
340 pH values compared with MK, following the same trend also in the binary systems where mix
341 M3 scored a higher value than mix M4 both at 28-d and 60-d.

342



343

344 **Figure 3.** (a) Compressive strength of MSWI FA S/S blocks at 28 and 60 days and TCLP

345 leachability of MSWI FA S/S blocks at (b) 28 and (c) 60 days (Leachability limits of trace

346 elements: 5 mg⁻¹ of As, 0.6 mg L⁻¹ of Cr, 0.2 mg⁻¹ of Cu, 0.75 mg L⁻¹ of Pb, 4.3 mg⁻¹ Zn)

347 (HK EPD, 2011).

348

349 As a result of the presence of aluminosilicate hydrates, AAMs reached a higher compressive
350 strength compared to the conventional scenario with OPC. This outcome demonstrates the great
351 potential of recycling MSWI FA into construction materials. However, field applications of
352 waste-derived AAMs are rare due to insufficient standards and guidelines.

353

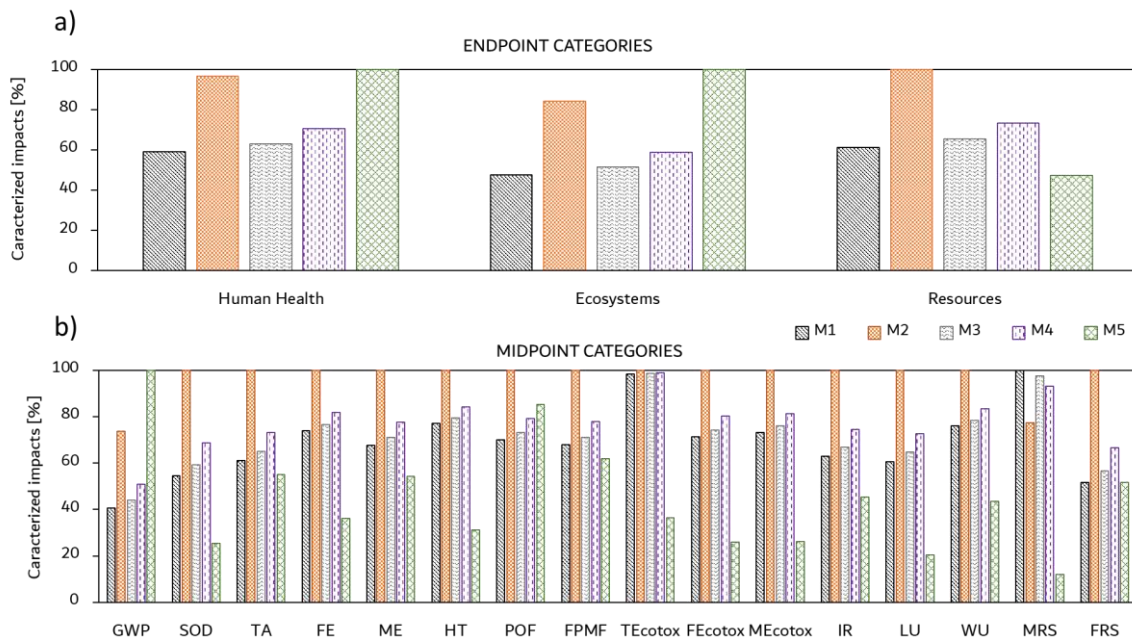
354 **3.2 LCA results**

355 The life cycle impacts of the considered MSWI FA S/S blocks are shown in Figs. 4a-b and
356 Table S4. The values are reported in percentage terms, normalized to the highest impact value
357 obtained for each category. In all the three endpoint categories (Fig. 4a), the mix M2 with MK
358 showed the highest impacts. The mix M1 with GGBS reached approximately comparable
359 values of the binary system M3, while the binary scenario M4 recorded higher impacts due to
360 a larger quantity of MK in the mix design. The conventional mix with OPC recorded the highest
361 impacts on human health and ecosystems categories but lower impacts on resources scarcity,
362 where instead mix M2 with MK scored the maximum.

363

364 From Fig. 4b, it is interesting to highlight that mix M1 with GGBS used as the precursor
365 reached the lowest impact values in various categories among all mixes. However, the mix with
366 OPC recorded comparable or even lower values in most categories, except for the impacts on
367 climate change, which were extremely high and equal to 292 kg CO₂eq (Table S4). Compared
368 to the traditional cement binder, a reduction of 60% in CO₂ emissions was obtained with mix
369 M1. This is in line with other LCA studies that estimated a reduction in GHGs between 40%
370 and 75% for AAMs (Bianco et al., 2021; Colangelo et al., 2021). Instead, mix M2 represented
371 the worst scenario in almost all the midpoint categories. This is ascribed to the energy-intensive
372 calcination process for metakaolin production (Habert and Ouellet-Plamondon, 2016) usually
373 in a temperature range of 500–950°C (Cheng et al., 2019). This agrees with the output by

374 Colangelo et al. (2021), where the scenario with MK produced three times the impacts related
 375 to the mix with GGBS in terms of GWP. It is noteworthy that the impacts on the category FRS
 376 at the midpoint level and Resources at the endpoint one are much lower for the conventional
 377 scenario with OPC, highlighting a non-correlation with climate change, despite the
 378 consumption of fossil resources accounted in the GWP. In fact, among all the emissions to air
 379 related to the clinker production process, which is included in the cement production, 0.84 kg
 380 of fossil carbon dioxide and 0.015 kg of biogenic carbon dioxide are emitted from every kg of
 381 produced clinker (Ecoinvent, 2016). Carbon dioxide released from cement manufacturing is
 382 mainly caused by the calcining process (removing CO₂ from limestone to form clinker)
 383 accounted for the 90% of the total CO₂eq, while the remaining is released during the burning
 384 of fuel in the kilns and other manufacturing processes (Huntzinger and Eatmon, 2009), as
 385 shown in the tree structure exported from SimaPro and presented in Figs. S3 and S6 in the
 386 Supplementary Materials.
 387



388
 389 **Figure 4.** Comparison of the environmental impacts in percentage of MSWI FA S/S blocks
 390 estimated with the (a) endpoint and (b) midpoint categories of ReCiPe 2016.

391

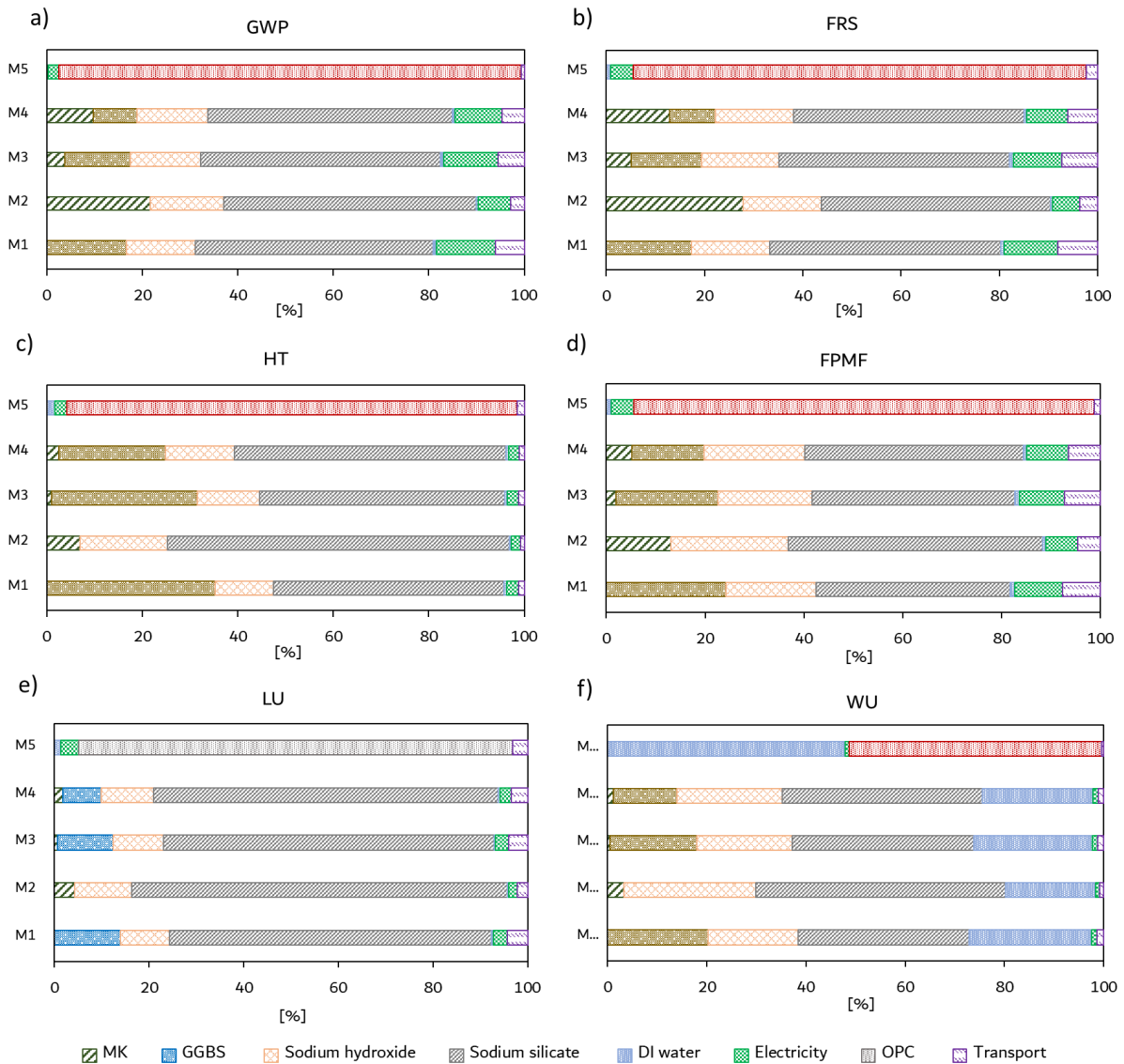
392 Figure 5 shows a contribution analysis with the most relevant midpoint categories with the
393 scope to identify each design's components responsible for the highest impacts. For all the
394 considered midpoint categories, the chemicals (sodium hydroxide and sodium silicate)
395 provided the highest contributions (always greater than 50%) to the total impacts of all mixes,
396 except for mix M5. It is evident that the tremendously high impact is related to the alkali
397 solution used in the AAMs, but particularly to water glass (Figs. S1, S2, S4, and S5). MK
398 recorded the highest contribution in GWP and FRS categories, underlining the footprint of the
399 calcination process (Figs. S2 and S5). GGBS contribution falls within the range 15–35%, with
400 the highest value in the HT category. Regarding mix M5, OPC production is the critical factor
401 responsible for the highest contributions to the total impacts. The electricity related to the
402 solution and paste mixing provided low contributions to the total impacts of all mixes, but the
403 highest percentage value was found for the category GWP, where mix M1 accounts for 10%
404 of the total. Also transport recorded low impacts for all categories, with the highest contribution
405 of 8% of the FRS in scenario M1. Using barges as the primary means of transport is highly
406 recommended, mainly because the average cargo capacity of a barge is generally 15 times
407 greater than one rail car and 60 times greater than one semi-trailer (Dry Cargo International,
408 2022). Size is the key to water transportation's efficiency, and it represents a real green
409 alternative to trucking. Lastly, the water consumption was higher in mix M5 where a higher
410 amount of water was used for mixing the paste, compared to scenarios M1, M2, M3, and M4
411 where an alkaline solution was required.

412

413 In line with Habert et al. (2011), this study highlights that the production of alkali-activated
414 blocks has more significant impacts on the midpoint categories than OPC-based blocks, except
415 for the GWP category. Other studies have reported similar concerns about the effects related

416 to sodium silicate production (Dal Pozzo et al., 2019). Although the highest impacts in most of
417 the categories are related to the chemicals used in the alkali solution, a properly-planned mix
418 design can help reduce the quantity of sodium silicate and sodium hydroxide necessary to
419 activate the precursors in the alkali-activated S/S treatment. In fact, according to the type of
420 aluminosilicate precursor, the higher the CaO content in the raw material, the less alkali-
421 activating solution is required. Therefore, GGBS is more sustainable compared to MK being
422 richer in CaO content (Wang et al., 2015). The low Si/Al ratio in MK-based AAMs means a
423 higher quantity of sodium silicate and water are required, leading to higher environmental
424 impacts (Juenger et al., 2019). Another research approach could be to use particle technology
425 more effectively, as proposed in the cement industry (Habert et al., 2011). Increasing particle
426 packing in the AAM mix would result in greater packing, requiring less active binder and alkali
427 solution (Provis et al., 2010).

428



429

430

Figure 5. Contribution analysis that all components provided to the total impacts of each

431

mix, estimated with the midpoint impact categories: (a) Global warming potential, (b) Fossil

432

resource scarcity, (c) Human toxicity, (d) Fine particulate matter formation, (e) Land use, and

433

(f) Water use.

434

4. Sensitivity analysis

435

Chemicals significantly influenced the results of alkali-activated blocks, as shown in Section

436

3.2. About 64–68% of the total GHGs emissions for block production are associated with

437

sodium silicate and sodium hydroxide (Fig. 5a). A sensitivity analysis thus plays an essential

438 role in estimating uncertainty and strengthening the reliability of the obtained results when
439 using different LCI input data for chemicals.

440

441 A sensitivity analysis following a one-at-a-time approach was carried out by varying chemical
442 production processes. A two-at-a-time approach was also included to identify the best
443 combination of production methods. Sodium silicate can be manufactured via furnace or
444 hydrothermal routes (Trabzuni et al., 2011). Regarding sodium hydroxide, three main different
445 production methods have been usually adopted worldwide: (i) membrane (MM), (ii) diaphragm
446 (DP), and (iii) mercury (MC) -based technologies. The membrane process is the most used and
447 has undoubtedly replaced MC and DP methods. An innovative version of the MM technology
448 is Oxygen Depolarized Cathode (ODC), and it represents a promising approach for reducing
449 the electricity demand (Jung et al., 2014). Further details about the above-mentioned
450 production systems can be found in Section 5.

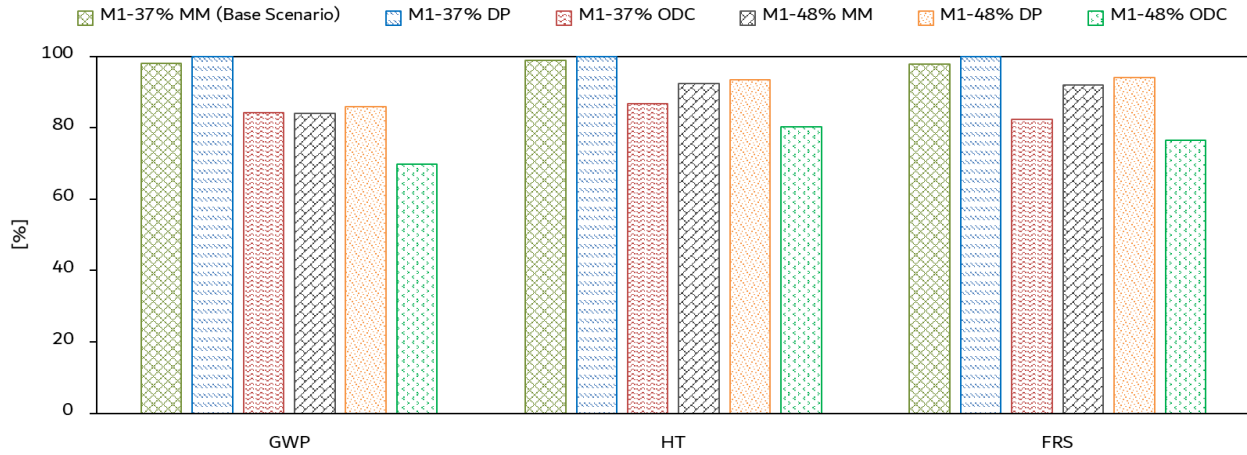
451

452 In this sensitivity analysis, alternative production scenarios were considered for both sodium
453 silicate ((i) 37% as base scenario, (ii) 48% as alternative route) and sodium hydroxide ((i) MM
454 as base scenario, (ii) DP as an alternative, (iii) ODC as an alternative). Mix M1 was used as
455 the base scenario since it represents the best alternative from the LCA study. It included sodium
456 silicate at a solution of 37% solid and sodium hydroxide produced via the MM production route.
457 In all the above-mentioned scenarios, Ecoinvent was used as the database for LCI-data except
458 for ODC chlor-alkali electrolysis, which is not globally available at a large scale yet. In this
459 last case, the study by Jung et al. (2014) was considered as reference, and a mass allocation
460 was used to define the environmental impacts associated with NaOH production. Table S5
461 shows the sensitivity analysis outcomes where the percentage difference for each midpoint
462 category was calculated in reference to the base scenario mix M1.

463

464 It is noteworthy that when sodium silicate is produced via the hydrothermal liquor route, almost
465 all the midpoint impacts decrease, with a reduction equal to -17%, -6.5%, -52%, -7% for GWP,
466 FRS, LU, HT, respectively (Fig. 6). However, WU recorded an increase of 16% compared to
467 the base scenario with the furnace liquor route. Regarding sodium hydroxide, the DP method
468 recorded slightly higher values than the base scenario, in a range of 0-2%, with a unique peak
469 of around +17% for WU category. The new innovative production route ODC-based recorded
470 the best results with a reduction of all the impacts, particularly -40%, -27%, -23%, respectively
471 for GWP, FRS, and HT of the base scenario with GGBS. In a direct comparison with mix M5
472 with OPC from Section 3.2, the scenario M1 48% - ODC, where two parameters have been
473 varied at the same time, can reduce the total GWP, FRS, and HT of -71%, -22%, and -24%,
474 respectively. These outcomes are novel and for the first time AAMs recorded better results not
475 only in GWP category but also in FRS and HT. This sheds light on the great value of AAMs
476 for the MSWI FA S/S treatment and underlines the importance of the production cycles of raw
477 materials.

478



479

480 **Figure 6.** Sensitivity analysis for alternative production scenarios for sodium silicate and
 481 sodium hydroxide for GWP, HT, and FRS midpoint categories.

482

483 **5. Alternative production methods for alkalis**

484 In order to achieve net-zero emissions by 2060 (Shi et al., 2021), the global goal is to create a
 485 decarbonized society as soon as possible, so that anthropogenic emissions (sources) and
 486 removals (sinks) of GHG can be balanced out (global carbon neutrality). Therefore, the choice
 487 of the best mix design and materials is a crucial step when evaluating a S/S treatment.

488

489 As described in Section 4, sodium silicate can be manufactured via furnace or hydrothermal
 490 route (Figs. 7a-b). In the furnace process, silicon sand and soda are melted at a temperature
 491 range of 1100–1200 °C to produce water glass directly, resulting in a high SiO₂/Na₂O molar
 492 ratio, and usually made available as an aqueous solution at ~37 wt.% (Passuello et al., 2017).
 493 Instead, in the hydrothermal process, an autoclave is used to dissolve sand in sodium hydroxide
 494 solution at 180-300°C resulting in sodium silicate with a lower SiO₂/Na₂O molar ratio and
 495 made available as a ~48 wt.% solution (Trabzuni et al., 2011). The energy consumption for
 496 furnace lumps dissolving and filtering in Ecoinvent is estimated to be 0.996 MJ/kg and 0.007

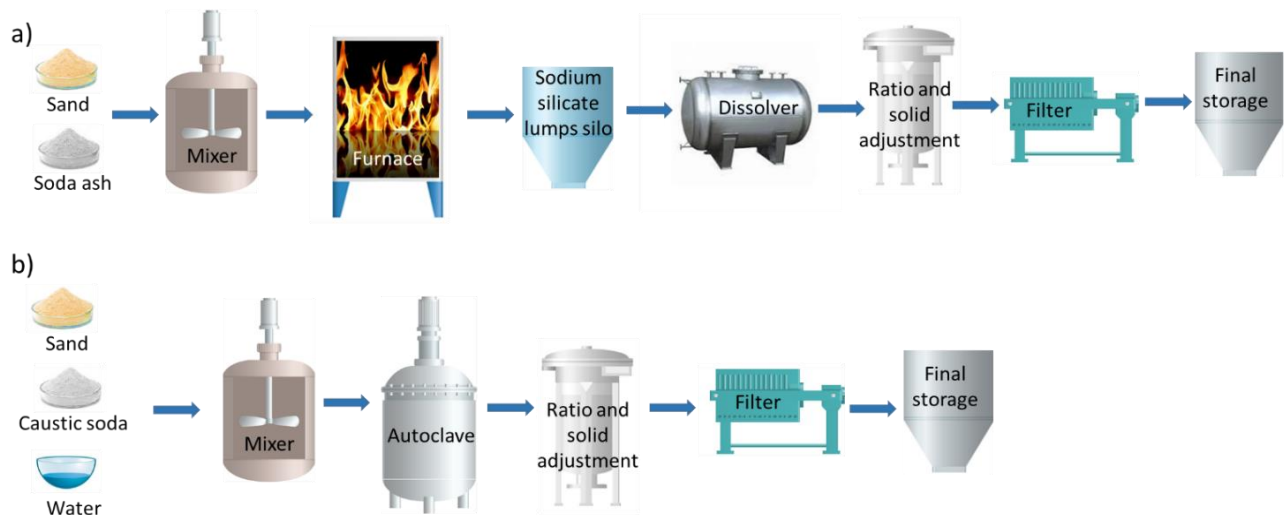
497 kWh/kg. This is slightly higher than the range 0.345-0.920 MJ/kg suggested by Fawer et al.
498 (1999). The second route involves hydrothermally dissolving silica sand in sodium hydroxide
499 solution. Reactions are conducted inside autoclaves, which are especially designed to handle
500 aggressive conditions. Upon filtering, a sodium silicate solution with a solid content of 48% is
501 obtained. In this case, 0.732 MJ/kg and 0.019 kWh/kg of output product are associated to this
502 production route in the database, falling in the range 0.350-0.680 MJ/kg suggested by Fawer
503 et al. (1999). The hydrothermal liquor production process appears to be more environmentally
504 friendly, especially in terms of global warming, land use, and human toxicity, but with higher
505 water consumption than the furnace liquor route.

506

507 Regarding sodium hydroxide, the membrane process is the most used (see Note S1) and it
508 allows operation at a lower clamping voltage, lower consumption of electrical energy and
509 steam, the possibility to change the current load on a daily basis, and minimization of
510 environmental contamination risk. ODC represents an innovative version of the MM
511 technology and a promising approach for reducing the electricity demand of chlor-alkali
512 electrolysis (Fig. 8). As a result of oxygen being introduced into the cathode, hydrogen
513 formation is suppressed and only chlorine and caustic soda are produced (Jung et al., 2014)
514 (Fig. 8c). However, future LCA studies should focus on developing a full-scale and globally
515 recognized database for ODC. This process has started to be used in the last decade, and it
516 represents the future for the production of chlorine and sodium hydroxide because it requires a
517 ten times reduced energy consumption, becoming more environmentally friendly and cost-
518 effective (Covestro Global Corporate, 2022; Jung et al., 2014).

519

520

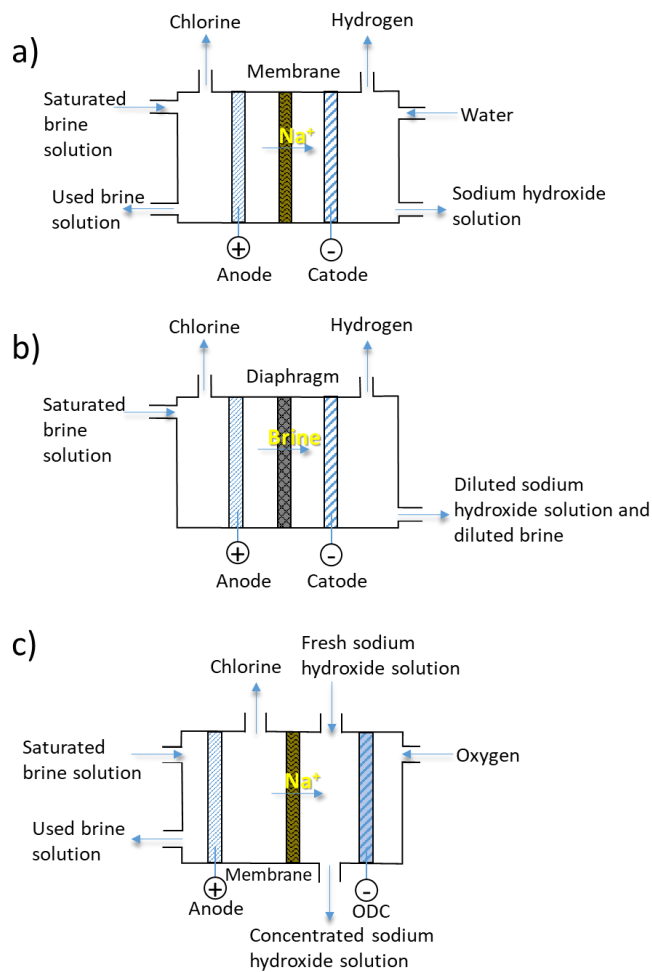


521

522

Figure 7. Sodium silicate production methods: (a) furnace and (b) hydrothermal routes.

523



524

525

Figure 8. Sodium hydroxide production methods: (a) membrane, (b) diaphragm, and (c) ODC

526

routes.

527

528 **Conclusions**

529 This paper aims to explore and develop alkali-activated mix designs for the S/S of MSWI FA,
530 alternatively to OPC. With 75% of MSWI FA, the blocks fulfilled the requirements for landfill
531 and reuse as fill materials. Overall, all the AAMs reached a higher strength than OPC.

532 The LCA revealed that the GGBS-based S/S treatment reduced by 60% GHG emissions
533 compared to the OPC treatment. However, since the production of both alkali-activators was
534 deemed the most critical unit process of the AAMs life, a focus on their production methods
535 was developed. The hydrothermal production route for sodium silicate showed lower impacts
536 than the furnace-based alternative, especially for land use and global warming. The membrane
537 production method was confirmed as the best option for sodium hydroxide. The ODC-based
538 membrane technology, revealed a substantial reduction of the impacts in every midpoint
539 category, mainly thanks to a reduced electricity demand for chlor-alkali electrolysis. Future
540 developments should focus on using alternative waste material as binders with suitable Si/Al
541 molar ratios in order to minimize the use of chemicals, but also on increasing the environmental
542 friendliness of chemicals production methods.

543

544 **Acknowledgements**

545 The authors appreciate the financial support from the Hong Kong Green Tech Fund
546 (GTF202020153).

547

548 **CRedit authorship contribution statement**

549 **Claudia Labianca:** Conceptualization, Methodology, Data curation, Formal analysis,
550 Investigation, Visualization, Writing—original draft. **Carmen Ferrara:** Investigation,
551 Methodology, Software, Validation, Writing—review & editing. **Yuying Zhang:** Data curation,

552 Validation, Writing–review & editing. **Xiaohong Zhu:** Data curation, Validation, Writing–
553 review & editing. **Giovanni De Feo:** Methodology, Supervision, Writing–review & editing.
554 **S.C Hsu:** Methodology, Software, Writing–review & editing. **Siming You:** Methodology,
555 Validation, Writing–review & editing. **Longbin Huang:** Conceptualisation, Validation,
556 Writing–review & editing. **Daniel C.W. Tsang:** Resources, Methodology, Supervision,
557 Project administration, Funding acquisition, Writing–review & editing.

558

559 **References**

- 560 Bajpai, R., Choudhary, K., Srivastava, A., Sangwan, K. S., Singh, M. 2020. Environmental
561 impact assessment of fly ash and silica fume based geopolymer concrete. *Journal of*
562 *Cleaner Production*, 254, 120147. <https://doi.org/10.1016/j.jclepro.2020.120147>
- 563 Bianco, I., Ap Dafydd Tomos, B., Vinai, R., 2021. Analysis of the environmental impacts of
564 alkali-activated concrete produced with waste glass-derived silicate activator – A LCA
565 study. *Journal of Cleaner Production* 316. <https://doi.org/10.1016/j.jclepro.2021.128383>
- 566 Billong, N., Oti, J., Kinuthia, J., 2021. Using silica fume based activator in sustainable
567 geopolymer binder for building application. *Construction and Building Materials* 275,
568 122177. <https://doi.org/10.1016/j.conbuildmat.2020.122177>
- 569 BS EN 12390. 2019. Testing Hardened Concrete Compressive Strength of Test Specimens.
570 British Standards Institution, London, UK.
- 571 Chen, L., Wang, L., Cho, D.W., Tsang, D.C.W., Tong, L., Zhou, Y., Yang, J., Hu, Q., Poon,
572 C.S., 2019a. Sustainable stabilization/solidification of municipal solid waste incinerator
573 fly ash by incorporation of green materials. *Journal of Cleaner Production* 222, 335–343.
574 <https://doi.org/10.1016/j.jclepro.2019.03.057>
- 575 Chen, L., Wang, L., Cho, D.W., Tsang, D.C.W., Tong, L., Zhou, Y., Yang, J., Hu, Q., Poon,
576 C.S., 2019b. Sustainable stabilization/solidification of municipal solid waste incinerator
577 fly ash by incorporation of green materials. *Journal of Cleaner Production* 222, 335–343.
578 <https://doi.org/10.1016/j.jclepro.2019.03.057>
- 579 Chen, L., Wang, L., Zhang, Y., Ruan, S., Mechtcherine, V., Tsang, D.C.W., 2022. Roles of
580 biochar in cement-based stabilization/solidification of municipal solid waste incineration
581 fly ash. *Chemical Engineering Journal* 430. <https://doi.org/10.1016/j.cej.2021.132972>

582 Cheng, H., Zhou, Y., Liu, Q., 2019. Kaolinite Nanomaterials: Preparation, Properties and
583 Functional Applications. *Nanomaterials from Clay Minerals: A New Approach to Green*
584 *Functional Materials* 285–334. <https://doi.org/10.1016/B978-0-12-814533-3.00006-5>
585 *China's Statistic Yearbook, 2020. China's Statistic Yearbook*
586 (<https://data.stats.gov.cn/easyquery.htm?cn=C01>) [WWW Document].

587 Chindaprasirt, P., Rattanasak, U., 2018. Fire-resistant geopolymer bricks synthesized from
588 high-calcium fly ash with outdoor heat exposure. *Clean Technologies and Environmental*
589 *Policy* 20, 1097–1103. <https://doi.org/10.1007/s10098-018-1532-4>

590 Cleary, J., 2013. Life cycle assessments of wine and spirit packaging at the product and the
591 municipal scale: a Toronto, Canada case study. *Journal of Cleaner Production* 44, 143–
592 151. <https://doi.org/10.1016/j.jclepro.2013.01.009>

593 Colangelo, F., Farina, I., Travaglioni, M., Salzano, C., Cioffi, R., Petrillo, A., 2021. Eco-
594 efficient industrial waste recycling for the manufacturing of fibre reinforced innovative
595 geopolymer mortars: Integrated waste management and green product development
596 through LCA. *Journal of Cleaner Production* 312, 127777.
597 <https://doi.org/10.1016/j.jclepro.2021.127777>

598 Contessi, S., Calgaro, L., Dalconi, M.C., Bonetto, A., Bellotto, M. Pietro, Ferrari, G.,
599 Marcomini, A., Artioli, G., 2020. Stabilization of lead contaminated soil with traditional
600 and alternative binders. *Journal of Hazardous Materials* 382, 120990.
601 <https://doi.org/10.1016/j.jhazmat.2019.120990>

602 Covestro Global Corporate, 2022. Energy-saving chlorine production (Accessed on the
603 22/04/2022 [https://www.covestro.com/en/sustainability/flagship-solutions/oxygen-](https://www.covestro.com/en/sustainability/flagship-solutions/oxygen-depolarized-cathode?msckid=09755175c21611ec9c0509934ab813b1)
604 [depolarized-cathode?msckid=09755175c21611ec9c0509934ab813b1](https://www.covestro.com/en/sustainability/flagship-solutions/oxygen-depolarized-cathode?msckid=09755175c21611ec9c0509934ab813b1)) [WWW
605 Document].

606 Dal Pozzo, A., Carabba, L., Bignozzi, M.C., Tugnoli, A., 2019. Life cycle assessment of a
607 geopolymer mixture for fireproofing applications. *International Journal of Life Cycle*
608 *Assessment* 24, 1743–1757. <https://doi.org/10.1007/s11367-019-01603-z>

609 Davidovits, J., 2009. *Geopolymer, Chemistry and Applications*. Lulu enterprises Inc.,
610 Morrisville, NC, USA, 574 [WWW Document]. URL
611 [https://scholar.google.com/scholar_lookup?title=Geopolymer%2C%20Chemistry%20an](https://scholar.google.com/scholar_lookup?title=Geopolymer%2C%20Chemistry%20an&d%20Applications&publication_year=2009&author=J.%20Davidovits)
612 [d%20Applications&publication_year=2009&author=J.%20Davidovits](https://scholar.google.com/scholar_lookup?title=Geopolymer%2C%20Chemistry%20an&d%20Applications&publication_year=2009&author=J.%20Davidovits) (accessed
613 4.22.22).

614 De Gisi, S., Todaro, F., Mesto, E., Schingaro, E., Notarnicola, M., 2020. Recycling
615 contaminated marine sediments as filling materials by pilot scale

616 stabilization/solidification with lime, organoclay and activated carbon. *Journal of Cleaner*
617 *Production* 269, 122416. <https://doi.org/10.1016/j.jclepro.2020.122416>

618 Del Valle-Zermeño, R., Formosa, J., Chimenos, J.M., Martínez, M., Fernández, A.I., 2013.
619 Aggregate material formulated with MSWI bottom ash and APC fly ash for use as
620 secondary building material. *Waste Management* 33, 621–627.
621 <https://doi.org/10.1016/j.wasman.2012.09.015>

622 Dry Cargo International, 2022. Cargo by rail and barge – cost-efficiency combines with
623 environmental protection [WWW Document]. URL
624 [https://www.drycargomag.com/cargo-by-rail-and-barge---cost-efficiency-combines-](https://www.drycargomag.com/cargo-by-rail-and-barge---cost-efficiency-combines-with-environmental-protection)
625 [with-environmental-protection](https://www.drycargomag.com/cargo-by-rail-and-barge---cost-efficiency-combines-with-environmental-protection) (accessed 4.8.22).

626 Dung, N.T., Unluer, C., 2017. Carbonated MgO concrete with improved performance: The
627 influence of temperature and hydration agent on hydration, carbonation and strength gain.
628 *Cement and Concrete Composites* 82, 152–164.
629 <https://doi.org/10.1016/j.cemconcomp.2017.06.006>

630 Ecoinvent, 2016. Cement, Portland, {RoW}|production|APOS, U. Swiss Centre for Life Cycle
631 Inventories.

632 Fan, C., Wang, B., Zhang, T., 2018. Review on cement stabilization/solidification of municipal
633 solid waste incineration fly ash. *Advances in Materials Science and Engineering* 2018.
634 <https://doi.org/10.1155/2018/5120649>

635 Fawer, M., Concannon, M., Rieber, W. 1999. LCA Case Studies LCI for the Production of
636 Sodium Silicate Life Cycle Inventories for the Production of Sodium Silicates.
637 <https://doi.org/10.1007/BF02979498>

638 GB/T 15581-2016. 2016. Emission standard of pollutants for caustic alkali and polyvinyl
639 chloride industry.

640 GB 34330, 2017. Identification Standards for Solid Wastes-General Rules. Ministry of
641 Environmental Protection, China.

642 Guo, B., Tan, Y., Wang, L., Chen, L., Wu, Z., Sasaki, K., Mechtcherine, V., Tsang, D.C., 2021.
643 High-efficiency and low-carbon remediation of zinc contaminated sludge by magnesium
644 oxysulfate cement. *Journal of Hazardous Materials* 408, 124486.
645 <https://doi.org/10.1016/j.jhazmat.2020.124486>

646 Habert, G., D’Espinoze De Lacaillerie, J.B., Roussel, N., 2011. An environmental evaluation
647 of geopolymers based concrete production: reviewing current research trends. *Journal of*
648 *Cleaner Production* 19, 1229–1238. <https://doi.org/10.1016/j.jclepro.2011.03.012>

649 Habert, G., Ouellet-Plamondon, C., 2016. Recent update on the environmental impact of
650 geopolymers. *RILEM Technical Letters* 1, 17–23.
651 <https://doi.org/10.21809/rilemtechlett.2016.6>

652 HJ 1134, 2020. Technical Specification for Pollution Control of Fly-ash from Municipal Solid
653 Waste Incineration. Ministry of Environmental Protection, China.

654 HK EPD, 2022. Integrated Waste Management Facilities, HK EPD [WWW Document]. URL
655 https://www.epd.gov.hk/epd/english/environmentinhk/waste/prob_solutions/WFdev_IW
656 [MF.html](https://www.epd.gov.hk/epd/english/environmentinhk/waste/prob_solutions/WFdev_IW) (accessed 3.23.22).

657 HK EPD, 2018. Tackling Imminent Waste Management Problem Integrated Waste
658 Management Facilities Environmental Protection Department, Hong Kong SAR
659 Government.

660 HK EPD, 2011. Practice Guide for Investigation and Remediation of Contaminated Land
661 Environmental Protection Department, Hong Kong SAR Government.

662 Hossain, M.U., Dong, Y., Ng, S.T., 2021. Influence of supplementary cementitious materials
663 in sustainability performance of concrete industry: A case study in Hong Kong. *Case*
664 *Studies in Construction Materials* 15, e00659.
665 <https://doi.org/10.1016/j.cscm.2021.E00659>

666 Hossain, M.U., Sohail, A., Ng, S.T., 2019. Developing a GHG-based methodological approach
667 to support the sourcing of sustainable construction materials and products. *Resources,*
668 *Conservation and Recycling* 145, 160–169.
669 <https://doi.org/10.1016/j.resconrec.2019.02.030>

670 Hossain, M.U., Wang, L., Chen, L., Tsang, D.C.W., Ng, S.T., Poon, C.S., Mechtcherine, V.,
671 2020. Evaluating the environmental impacts of stabilization and solidification
672 technologies for managing hazardous wastes through life cycle assessment: A case study
673 of Hong Kong. *Environment International* 145, 106139.
674 <https://doi.org/10.1016/j.envint.2020.106139>

675 Huijbregts, M.A.J., Steinmann, Z.J.N., Elshout, P.M.F., Stam, G., Verones, F., Vieira, M., Zijp,
676 M., Hollander, A., van Zelm, R., 2017. ReCiPe2016: a harmonised life cycle impact
677 assessment method at midpoint and endpoint level. *International Journal of Life Cycle*
678 *Assessment* 22, 138–147. <https://doi.org/10.1007/s11367-016-1246-y>

679 Huntzinger, D.N., Eatmon, T.D., 2009. A life-cycle assessment of Portland cement
680 manufacturing: comparing the traditional process with alternative technologies. *Journal*
681 *of Cleaner Production* 17, 668–675. <https://doi.org/10.1016/j.jclepro.2008.04.007>

682 ISO, 2006. ISO 14040: Environmental management: life cycle assessment, principles and
683 guidelines. International Organization for Standardization, Geneva.

684 Jeremiah, J.J., Abbey, S.J., Booth, C.A., 2021. Geopolymers as Alternative Sustainable Binders
685 for Stabilisation of Clays — A Review. *Geotechnics*, 1(2), 439-459.
686 <https://doi.org/10.3390/geotechnics1020021>

687 Jin, M., Zheng, Z., Sun, Y., Chen, L., Jin, Z., 2016. Resistance of metakaolin-MSWI fly ash
688 based geopolymer to acid and alkaline environments. *Journal of Non-Crystalline Solids*
689 450, 116–122. <https://doi.org/10.1016/j.jnoncrysol.2016.07.036>

690 Juenger, M.C.G., Snellings, R., Bernal, S.A., 2019. Supplementary cementitious materials:
691 New sources, characterization, and performance insights. *Cement and Concrete Research*.
692 <https://doi.org/10.1016/j.cemconres.2019.05.008>

693 Jung, J., Postels, S., Bardow, A., 2014. Cleaner chlorine production using oxygen depolarized
694 cathodes? A life cycle assessment. *Journal of Cleaner Production* 80, 46–56.
695 <https://doi.org/10.1016/j.jclepro.2014.05.086>

696 Kanhar, A.H., Chen, S., Wang, F., 2020. Incineration Fly Ash and Its Treatment to Possible
697 Utilization : A Review. *Energies*, 13(24), 6681. <https://doi.org/10.3390/en13246681>

698 Krivenko, P., 2017. Why Alkaline Activation-60 Years of the Theory and Practice of Alkali-
699 Activated Materials. Article in *Journal of Ceramic Science and Technology* 323–334.
700 <https://doi.org/10.4416/jcst2017-00042>

701 Li, Y., Min, X., Ke, Y., Liu, D., Tang, C., 2019(a). Preparation of red mud-based geopolymer
702 materials from MSWI fly ash and red mud by mechanical activation. *Waste Management*
703 83, 202–208. <https://doi.org/10.1016/j.wasman.2018.11.019>

704 Li, N., Shi, C., Zhang, Z., 2019(b). Understanding the roles of activators towards setting and
705 hardening control of alkali-activated slag cement. *Composites Part B: Engineering* 171,
706 34–45. <https://doi.org/10.1016/j.compositesb.2019.04.024>

707 McLellan, B.C., Williams, R.P., Lay, J., Van Riessen, A., Corder, G.D., 2011. Costs and carbon
708 emissions for geopolymer pastes in comparison to ordinary portland cement. *Journal of*
709 *Cleaner Production* 19, 1080–1090. <https://doi.org/10.1016/j.jclepro.2011.02.010>

710 Passuello, A., Rodríguez, E.D., Hirt, E., Longhi, M., Bernal, S.A., Provis, J.L., Kirchheim, A.P.,
711 2017. Evaluation of the potential improvement in the environmental footprint of
712 geopolymers using waste-derived activators. *Journal of Cleaner Production* 166, 680–689.
713 <https://doi.org/10.1016/j.jclepro.2017.08.007>

714 Patrisia, Y., Law, D. W., Gunasekara, C., Wardhono, A. 2022. Life cycle assessment of alkali-
715 activated concretes under marine exposure in an Australian context. *Environmental*
716 *Impact Assessment Review*, 96, 106813. <https://doi.org/10.1016/j.eiar.2022.106813>

717 PRé Consultants, 2019. SimaPro 9.0049 version. PRé Consultants, The Netherlands.

718 Provis, J.L., Arbi, K., Bernal, S.A., Bondar, D., Buchwald, A., Castel, A., Chithiraputhiran, S.,
719 Cyr, M., Dehghan, A., Dombrowski-Daube, K., Dubey, A., Ducman, V., Gluth, G.J.G.,
720 Nanukuttan, S., Peterson, K., Puertas, F., van Riessen, A., Torres-Carrasco, M., Ye, G.,
721 Zuo, Y., 2019. RILEM TC 247-DTA round robin test: mix design and reproducibility of
722 compressive strength of alkali-activated concretes. *Materials and Structures/Materiaux et*
723 *Constructions* 52, 1–13. <https://doi.org/10.1617/s11527-019-1396-z>

724 Provis, J.L., Duxson, P., van Deventer, J.S.J., 2010. The role of particle technology in
725 developing sustainable construction materials. *Advanced Powder Technology* 21, 2–7.
726 <https://doi.org/10.1016/j.apr.2009.10.006>

727 Puligilla, S., Chen, X., Mondal, P. 2019. Does synthesized CSH seed promote nucleation in
728 alkali activated fly ash-slag geopolymer binder?. *Materials and Structures*, 52(4), 1-13.
729 <https://doi.org/10.1617/s11527-019-1368-3>

730 Qiang, T., Heejong, K., Kazuto, E., Takeshi, K., Toru, I., 2015. Size effect on lysimeter test
731 evaluating the properties of construction and demolition waste leachate. *Soils and*
732 *Foundations* 55, 720–736. <https://doi.org/10.1016/j.sandf.2015.06.005>

733 Rashad, A.M., 2013. Alkali-activated metakaolin: A short guide for civil Engineer – An
734 overview. *Construction and Building Materials* 41, 751–765.
735 <https://doi.org/10.1016/j.conbuildmat.2012.12.030>

736 Robayo-Salazar, R., Mejía-Arcila, J., de Gutiérrez, R. M., Martínez, E. 2018. Life cycle
737 assessment (LCA) of an alkali-activated binary concrete based on natural volcanic
738 pozzolan: A comparative analysis to OPC concrete. *Construction and Building Materials*,
739 176, 103-111. <https://doi.org/10.1016/j.conbuildmat.2018.05.017>

740 Salas, D.A., Ramirez, A.D., Ulloa, N., Baykara, H., Boero, A.J., 2018. Life cycle assessment
741 of geopolymer concrete. *Construction and Building Materials* 190, 170–177.
742 <https://doi.org/10.1016/j.conbuildmat.2018.09.123>

743 Shi, X., Zhang, C., Liang, Y., Luo, J., Wang, X., Feng, Y., Li, Y., Wang, Q., Abomohra, A.E.F.,
744 2021. Life cycle assessment and impact correlation analysis of fly ash geopolymer
745 concrete. *Materials* 14. <https://doi.org/10.3390/MA14237375>

746 Singh, N.B., Kumar, M., Rai, S., 2020. Geopolymer cement and concrete: Properties. *Materials*
747 *Today: Proceedings* 29, 743–748. <https://doi.org/10.1016/j.matpr.2020.04.513>

748 Sun, K., Peng, X., Wang, S., Zeng, L., Ran, P., Ji, G., 2020. Effect of nano-SiO₂ on the
749 efflorescence of an alkali-activated metakaolin mortar. *Construction and Building*
750 *Materials* 253, 118952. <https://doi.org/10.1016/j.conbuildmat.2020.118952>

751 Teh, S. H., Wiedmann, T., Castel, A., de Burgh, J., 2017. Hybrid life cycle assessment of
752 greenhouse gas emissions from cement, concrete and geopolymer concrete in Australia.
753 *Journal of cleaner production*, 152, 312-320.
754 <https://doi.org/10.1016/j.jclepro.2017.03.122>

755 Trabzuni, F.M.S., el Dekki, H.M., Gopalkrishnan, C.C., 2011. Process for Hydrothermal
756 Production of Sodium Silicate Solutions and Precipitated Silicas. U.S. Patent No.
757 8,057,770. Washington, DC.

758 US EPA, 2019. Guidelines for Human Exposure Assessment (EPA/100/B-19/001)// Risk
759 Assessment Forum. Washington, DC, U.S. Environmental Protection Agency.

760 Wang, L., Chen, L., Cho, D.W., Tsang, D.C.W., Yang, J., Hou, D., Baek, K., Kua, H.W., Poon,
761 C.S., 2019. Novel synergy of Si-rich minerals and reactive MgO for
762 stabilisation/solidification of contaminated sediment. *Journal of Hazardous Materials* 365,
763 695–706. <https://doi.org/10.1016/j.jhazmat.2018.11.067>

764 Wang, S. D., Pu, X. C., Scrivener, K. L., Pratt, P. L. (1995, published online on 2015). Alkali-
765 activated slag cement and concrete: a review of properties and problems. *Advances in*
766 *cement research*, 7(27), 93-102. <http://dx.doi.org/10.1680/adcr.1995.7.27.93> 7, 93–102.

767 Xue, Y., Liu, X. 2021. Detoxification, solidification and recycling of municipal solid waste
768 incineration fly ash: A review. *Chemical Engineering Journal*, 420, 130349.
769 <https://doi.org/10.1016/j.cej.2021.130349>

770 Yakubu, Y., Zhou, J., Ping, D., Shu, Z., Chen, Y., 2018. Effects of pH dynamics on
771 solidification/stabilization of municipal solid waste incineration fly ash. *Journal of*
772 *Environmental Management* 207, 243–248.
773 <https://doi.org/10.1016/j.jenvman.2017.11.042>

774 Yip, C. K., Van Deventer, J. S. J. 2003. Microanalysis of calcium silicate hydrate gel formed
775 within a geopolymeric binder. *Journal of Materials Science*, 38(18), 3851-3860.
776 <https://doi.org/10.1023/A:1025904905176>

777 Zhang, Yuying, Wang, L., Chen, L., Ma, B., Zhang, Yike, Ni, W., Tsang, D.C.W., 2021.
778 Treatment of municipal solid waste incineration fly ash: State-of-the-art technologies and
779 future perspectives. *Journal of Hazardous Materials* 411, 125132.
780 <https://doi.org/10.1016/j.jhazmat.2021.125132>

781